PROCEEDINGS OF SCIENCE

Axes of discovery: The time variable Universe

James Cordes[*†]
Cornell University
E-mail: jmc33@cornell.edu

As Heraclitus might have said, "You don't observe the same universe twice." In modern times we recognize the time domain as an important dimension in the overall phase space of variables that characterizes the observable universe. Examples of time-dependent sources abound across the electromagnetic spectrum and in non-photonic regimes (neutrinos, gravitational waves, cosmic rays). This paper discusses both known and speculative aspects of the radio transient sky, with an emphasis on discoveries that can be made with new, appropriately designed instrumentation and telescopes. Known source classes include planets, flare stars, brown dwarfs, pulsars, magnetars, masers, supernovae and gamma-ray burst afterglows. Hypothetical classes include additional planetary emissions, ETI emissions (including radar signals to aid mitigation of orbital debris impacts), evaporating black holes, hyper-giant pulses from neutron stars rotating near breakup, and prompt gamma-ray bursts. Nature undoubtedly has a longer list! A generalized survey figure of merit is presented that takes into account the rate and duration of transient celestial events. The key for expanding discovery space is a wide field of view (FoV) combined with adequate sensitivity and high-resolution sampling in the combined time-frequency domain. Implementation of time-frequency processing is an integral part of synoptic survey modes for existing and forthcoming radio telescopes that can allow commensal observations of steady sources (e.g. HI from galaxies) along with transient sources. Time-frequency processing is needed in all cases for calibration and excision of radio-frequency interference. The Square Kilometer Array (SKA), in particular, can be a powerful radio synoptic survey telescope (RSST) that has tremendous potential as a discovery instrument and for cross-wavelength and joint photonic/non-photonic studies.

From Planets to Dark Energy: the Modern Radio Universe
October 1-5 2007
The University of Manchester, UK

[*]Speaker.
[†]Work supported by the US National Science Foundation

PoS(MRU)035

1. Introduction

Time variability is a tool for studying astrophysical objects themselves and for probing intervening media and spacetime. The transient sky is on the astrophysical frontier across the entire electromagnetic spectrum and also in non-photonic regimes, including cosmic rays and gravitational waves. The transient sky at high photon energies has been explored much more than in other bands, as evidenced by the great successes of wide field-of-view instruments in finding gamma-ray bursts, accreting sources and bursting pulsars over the last forty years. The next large gamma-ray facility, GLAST (the Gamma-ray Large Area Space Telescope) will survey the entire sky every three hours for at least its first year of operation, allowing a comprehensive inventory of both steady and variable sources.

At optical wavelengths, searches for gravitational microlensing events and for Type Ia supernovae have driven the development of high throughput optical telescopes. Forthcoming instruments building upon these successes include PanSTARRs (Panoramic Survey Telescope and Rapid Response System) and the Large Synoptic Survey Telescope (LSST/LST)[1].

This paper discusses the transient radio sky. Examples of transient radio signals are known that range from 0.4 ns and longer in time scale with apparent brightness temperatures from thermal to 10^{42}K. However, compared to the high-energy transient sky, we know next to nothing about the overall constituency of the transient radio sky. A highlighted science area for the Square Kilometer Array (SKA) is "Exploration of the Unknown" [23] which includes the overall phase space opened up by the SKA and the likely discovery of new classes of objects and phenomena. Another chapter in the SKA science book [9] discusses the anticipated payoff from an SKA design that combines widefield sampling of the sky with high sensitivity and flexibility in analyzing likely or hypothetical event signatures and time scales. Transient radio signals provide not only unique windows into radio sources themselves, but are superb diagnostics of densities and magnetic fields in intervening media, including the interstellar medium and the intergalactic medium.

Most known radio transients have been found by making radio observations on targets selected from other surveys, including those made at other wavelengths or energies, such as the intermittent pulsar B1931+24 [17], radio afterglows from gamma-ray burst (GRB) sources, the turn-on of periodic radio pulsations from a formerly quiescent magnetar, J1810-197 [5, 6], and the detection of repeating (if not periodic) pulses from a brown dwarf [12]. Recent exceptions include the discovery of the rotating radio transient (RRAT) population [20] and transient sources in the Galactic-center (GC) direction [2, 16] found through VLA imaging observations of the GC. It is clear that blind surveys of the transient sky will yield new objects and new classes of objects that will serve as laboratories for the basic physics of extreme states of matter as well as providing an inventory of Nature's proclivity for astrophysical complexity. Indeed, Nature is said to abhor a vaccuum, and this appears to be true in parameter space as well as physical space.

Given the wide diversity of signal types among known radio transients and recognizing that new

[1]This particular name is not informative as to the wavelength and would be better changed by adding an "O" for optical to the acronym.

classes of transients remain to be discovered, our discussion focuses on how best to sample both slow and fast transients in blind surveys. Pioneering work has been done with the 13-beam system on the Parkes telescope and with the 7-beam ALFA system on the Arecibo telescope. Transient surveys are part of the stated science cases for essentially all planned radio telescopes, including the SKA and pathfinders for the SKA and related projects, including the Allen Telescope Array (ATA, Hat Creek), LOFAR (the low-frequency array, Netherlands), the Long Wavelength Array (LWA, Southwest US), the Mileura Widefield Array (MWA in Australia), MeerKAT (the Karoo Array Telescope in South Africa), and the Australia SKA Pathfinder (ASKAP).

2. Radio Transients

Nature can be profligate in producing radio photons and turn sources into bright, easily-detectable radio beacons. Under appropriate conditions, this occurs via coherent radiation processes that yield N^2 rather than N times the radiation of a single particle in an N-particle system. In most sources, radio emission is not the dominant energy channel for dumping free energy but it is an extremely significant information channel. Examples include pulsars and radio pulses from ultra high-energy cosmic rays.

2.1 Transient Phase Space

Giant pulses from radio pulsars are prototypes for fast transients along with solar bursts and flare stars, while sources such as microquasars and gamma-ray burst (GRB) afterglows exemplify longer-duration transients. We may use these sources as initial guides for specifying blind-survey parameters. However, simple observational phase space arguments suggest that *instantaneous coverage of a large fraction of the sky with appropriate sampling of the frequency-time plane will yield a rich variety of transient sources, including new classes of objects*. Figure 1 shows the phase space of pulse width W against flux density. Lines of constant brightness temperature are calculated assuming that W is the light-travel time across the source,

$$T_b = \frac{S}{2k}\left(\frac{D}{\nu W}\right)^2 = 10^{20.5}\,\mathrm{K}\,S_{\mathrm{mJy}}\left(\frac{D_{\mathrm{kpc}}}{\nu_{\mathrm{GHz}}W_{\mathrm{ms}}}\right)^2, \tag{2.1}$$

where S_{mJy} is the peak flux density (mJy) at frequency ν (GHz) and D is the distance (kpc). For some sources W can be much smaller than the light travel time owing to relativistic compression.

It is useful to classify the wide range of known time scales in terms of how they are best sampled empirically. *Slow transients* are defined as those with time scales longer than the time it takes to image the relevant region of the sky (e.g. the Galactic plane, the Galactic center, or the entire sky), either in a single pointing or as a mosaic or raster scan. Detection of such objects can be accomplished simply through repeated mapping of the sky and thus does not require special capabilities beyond those needed for imaging applications. Depending on survey speed, transients of days or more may be considered slow. GRBs are currently detected at $\gtrsim 100\,\mu$Jy levels using the VLA at frequencies of 5 and 8 GHz [11]. The full SKA could detect GRB afterglows up to 100 times fainter levels.

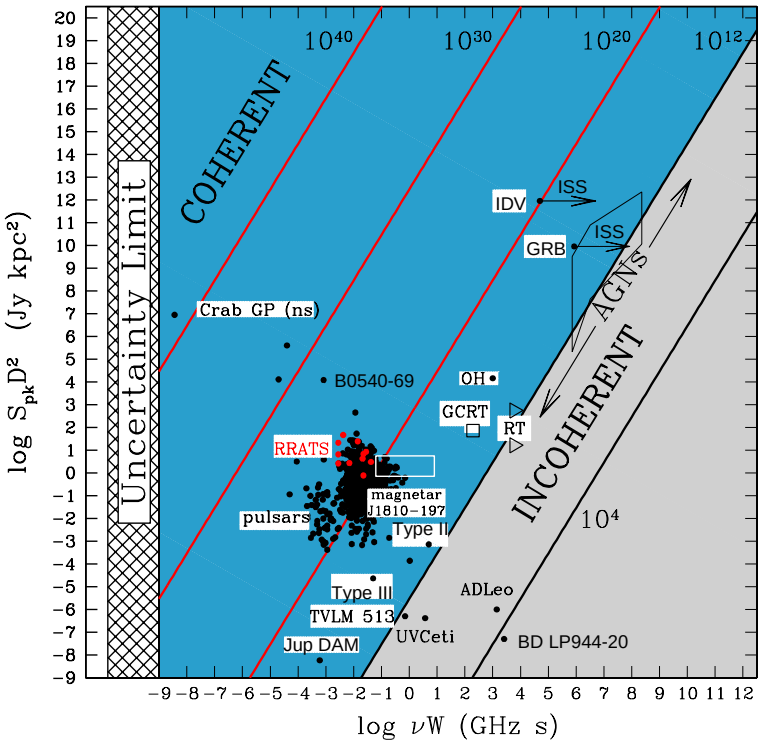

Figure 1: Time-luminosity phase space for known radio transients, a log-log plot of the product of peak flux $S_{\rm pk}$ in Jy and the square of the distance D in kpc vs. the product of frequency ν in GHz and pulse width W in s. The "uncertainty" limit on the left indicates that $\nu W \gtrsim 1$ as follows from the uncertainty principle. Lines of constant brightness temperature $T = SD^2/2k(\nu W)^2$ are shown, where k is Boltzmann's constant. Points are shown for the 'nano-giant' pulses detected from the Crab [14], giant pulses detected from the Crab pulsar and a few millisecond pulsars, and single pulses from other pulsars. Points are shown for Jovian and solar bursts, flares from stars, brown dwarfs (e.g. TVLM 513-46546 [12]), OH masers, and AGNs. The regions labeled 'coherent' and 'incoherent' are separated by the canonical 10^{12}K limit from the inverse Compton effect that is relevant to incoherent synchrotron sources. Arrows pointing to the right for the GRB and intra-day variable (IDV) points indicate that interstellar scintillation (ISS) implies smaller brightness temperatures than if characteristic variation times are used to estimate the brightness temperature. The growing number of recent discoveries of transients illustrates the fact that empty regions of the $\nu W - S_{\rm pk}D^2$ plane may be populated with sources not yet discovered. Recent discoveries include the "rotating radio transients" (RRATs) [20], the Galactic center transient source, GCRT J1745-3009 [16], the bright, bursting magnetar XTE J1810-197 [5], and recently discovered transients (labelled "RT") associated with distant galaxies [3]. The rightward-directed triangles used to mark the two RT sources indicate that the transient durations are only known to be longer than ~ 20 min.

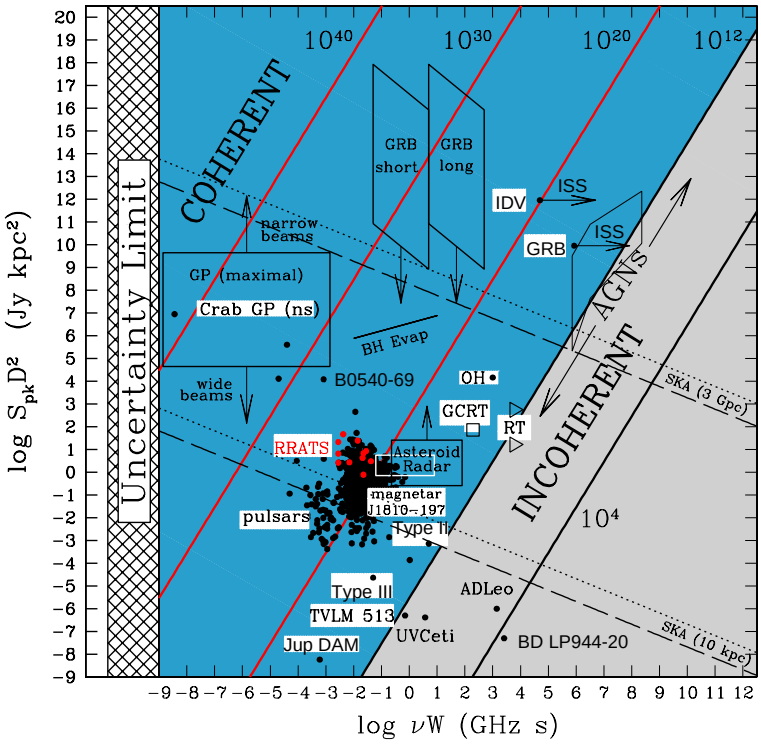

Figure 2: Same as previous figure but also including hypothetical transient sources and detection curves. Possible transients include maximal giant-pulse emission from pulsars, prompt radio emission from GRBs, bursts from evaporating black holes, and radar signals used to track potentially impacting asteroids and comets. Dashed lines indicate the detection threshold for the full SKA for sources at distance of 10 kpc and 3 Gpc. Dotted lines correspond to a 10% SKA, comparable to the Arecibo telescope. At a given νW, a source must have luminosity above the line to be detectable. The curves assume optimal detection (matched filtering).

Fast transients, conversely, are those that would be missed in the time it takes to scan the sky, leading to incompleteness of the survey. Sub-second transients are linked to coherent radiation and, in many cases, to compact sources in extreme matter states. They also are affected by plasma propagation effects, such as dispersion and multipath scattering that can distort pulses and inhibit detection. By the same token, such transients are excellent probes of the intervening interplanetary, interstellar and intergalactic media. Fast transients require the same observing modes and post-processing as for pulsars. The Crab pulsar is the most extreme known case in showing temporal structure down to ~ 0.4 ns scales [14] and giant pulses that exceed 100 times the entire flux density of the Crab Nebula. Pulsars and giant-pulse emission are prototypes for coherent radiation that may originate from other high-energy objects in which collimated particle flows can drive plasma instabilities necessary for coherent radiation. Examples include prompt radio burst emission from GRB-type sources, perhaps even from gamma-ray quiet objects; flare stars, jovian-burst like radiation from planets, AGNs, and merging neutron stars at cosmological distances [15], some of

which we designate in Figure 2. Photon reprocessing may limit the radio brightness of GRBs, so significant non-detections will constrain source conditions [19].

Using GRBs as a guide, it may be noted that the rate of GRB detection with gamma-ray instruments has relied more on instantaneous wide-field sky coverage than on sensitivity. The same statement holds for the detection of prompt optical emission at $m_v = 9$ in at least one case [1]. For this reason, we suggest that use of subarray modes to increase the instantaneous sky coverage — at less than full sensitivity — will be productive in surveying the transient radio sky.

2.2 Propagation Effects

Intervening plasmas are the dominant causes of effects that modify radio emission from both steady and time-dependent sources. Of course plasma effects are accompanied by gravitatational lensing and redshift-dependent phenomena on cosmological lines of sight.

Dispersion: Fast transients have signal shapes modified by the strongly frequency-dependent travel time. When a pulse propagates dispersively, its arrival time varies with frequency as $\Delta t = 4.15\ \mathrm{ms}\ \mathrm{DM}\nu^{-2}$ for dispersion measure DM (the line-of-sight integral of electron density) in standard units (pc cm^{-3}) and ν in GHz. Equivalently, the sweep rate in frequency is $\dot{\nu} \propto \nu^3 \mathrm{DM}^{-1}$. If not compensated, a pulse measured across a finite bandwidth is smeared out. However, dedispersion techniques are well developed, allowing this deterministic effect to be largely mitigated. *A priori* DM is not known, so trial values must be used from a set of plausible values. For Galactic sources, DM ranges between 2.4 and ~ 1300 pc cm^{-3} among known pulsars. The NE2001 model for free electrons in the Galaxy [8] predicts dispersion measures up to about 3400 pc cm^{-3} when looking through the Galactic center region. However, much larger values will obtain for lines of sight that pierce dense HII regions.

Extragalactic sources will show contributions to DM from foreground Galactic electrons as well as from a host or intervening galaxy (if relevant) and from the intergalactic medium. A fiducial value for intergalactic dispersion is

$$\mathrm{DM_{igm}} = \mathrm{cH_0^{-1} n_{e0}} \approx 10^3\ \mathrm{pc\ cm^{-3}}, \tag{2.2}$$

where n_{e0} is the electron density associated with the baryonic fraction of the total closure density.

Scattering and Scintillation: Multipath propagation along Galactic lines of sight occurs because there is fine scale structure in the free electrons, down to scales $\sim 10^3$ km (e.g. [22]), from which radio waves diffract and refract. Relevant effects include angular broadening ("seeing"), pulse broadening, and intensity scintillations.

Measured pulse broadening on Galactic lines of sight is as large as ~ 1 s but scales very strongly with frequency, $\tau_d \propto \nu^{-4}$. On lines of sight to the Galactic center, τ_d is hundreds of seconds at 1 GHz and prohibits the detection of pulsars around Sgr A* at conventional frequencies used in pulsar searches. Searches for fast transients from the Galactic center region therefore must be done at high frequencies $\gtrsim 10$ GHz.

Diffractive scintillation (DISS) results from interference between scattered wavefronts and produces structure in both time and frequency with representative scales of 100 s and 0.1 MHz, but with ranges in each of many orders of magnitude. Refractive scintillation (RISS) is caused by focusing and defocusing of radiation from scales much larger than those responsible for DISS in the strong-scattering regime. RISS is broadband, $\Delta\nu/\nu \sim 1$, and has time scales of hours and longer, depending on the line of sight. RISS from Galactic plasma appears to underly the "intraday variability" (IDV) of some active galactic nuclei (see Jauncey's paper, these proceedings).

Broadening of pulses from extragalactic sources by intergalactic or extragalactic plasma has not yet been measured definitively (but see further discussion below). Propagation through a face-on intervening galaxy like the Milky Way would scatter radiation into ~ 1 mas at 1 GHz and broaden a pulse by a fiducial broadening time

$$\Delta t_{\rm face\ on} = \frac{\theta_s^2}{2H_0} = 5\theta_{\rm s,mas}^2\ {\rm sec.} \tag{2.3}$$

Pulse broadening could be much larger, however, from edge-on and starburst galaxies and the intergalactic medium (IGM), if turbulent like the interstellar medium, could also make a sizable contribution. Detection of pulses from cosmological sources would give a very powerful tool for probing the IGM as would relatively nearby sources in local-group galaxies.

2.3 Detectability

The signal-to-noise ratio for a pulse after matched filtering (including dedispersion for fast transients) is

$$\frac{S}{N} = \frac{S(N_{\rm pol}BW)^{1/2}}{S_{\rm sys}}, \tag{2.4}$$

where S is the peak flux density, $N_{\rm pol}$ is the number of polarization channels, B is the bandwidth, and W is the pulse width (FWHM); $S_{\rm sys}$ is the system-equivalent flux density (SEFD) that we assume to be 0.14 Jy for the SKA[2] and 3 Jy for Arecibo at 1.4 GHz. Requiring $S/N > m = 10$ and using nominal parameters for Arecibo and the SKA we get a minimum detectable flux density

$$S_{\rm min,SP} = \left(\frac{m}{10}\right)\left(\frac{1\,{\rm ms}}{W}\right)^{1/2}\left(\frac{1\,{\rm GHz}}{B}\right)^{1/2} \times \begin{cases} \dfrac{21\,{\rm mJy}}{g_\theta} & {\rm AO} \\ \dfrac{0.98\,{\rm mJy}}{g_\theta f_{\rm c}} & {\rm SKA,} \end{cases} \tag{2.5}$$

[2]The value for the SKA is based on the original specification of $A_{\rm eff}/{\rm T_{sys}} = 2\times10^4$ m^2 K^{-1} for the full array. Recently, the specification has been reduced to 60% of this value. Moreover, with a wide range of baselines, not all the sensitivity will be usable in blind, widefield surveys. We account for this latter issue by introducing the factor f_c, the fraction of the sensitivity in a core array that can be used for widefield surveys.

where $g_\theta \leq 1$ accounts for the off-axis gain being less than assumed and f_c is defined in the footnote. The minimum flux density corresponds to a minimum brightness temperature

$$T_{\rm min,SP} = \left(\frac{m}{10}\right)\left(\frac{1\,{\rm ms}}{W}\right)^{5/2}\left(\frac{1\,{\rm GHz}}{B}\right)^{1/2}\left(\frac{D_{\rm kpc}}{\nu_{\rm GHz}}\right)^{2} \times \begin{cases} \dfrac{10^{21.8}{\rm K}}{g_\theta} & {\rm AO} \\ \dfrac{10^{20.5}{\rm K}}{g_\theta\, f_{\rm c}} & {\rm SKA,} \end{cases} \tag{2.6}$$

A burst of amplitude $S_{\rm pk}$ from a known source at distance $D = D_{\rm kpc}$ kpc can be detected to a maximum distance

$$\begin{aligned} D_{\rm max} &= D\left(\frac{S_{\rm pk}}{S_{\rm min,SP}}\right)^{1/2} \\ &= D_{\rm kpc}\left(\frac{S_{\rm pk}}{1\ {\rm Jy}}\right)^{1/2}\left(\frac{10}{m}\right)^{1/2}\left(\frac{W}{1\,{\rm ms}}\right)^{1/4}\left(\frac{B}{1\,{\rm GHz}}\right)^{1/4} \times \begin{cases} 6.9\ {\rm kpc}\, g_\theta^{1/2} & {\rm AO} \\ 32\ {\rm kpc}\,(g_\theta\, f_{\rm c})^{1/2} & {\rm SKA.} \end{cases} \end{aligned} \tag{2.7}$$

The SKA can see about 1.5 orders of magnitude fainter than Arecibo. However, the much greater advantage of the SKA over Arecibo will consist of the sky coverage and greater resilience against radio-frequency interference (RFI). With such coverage we can expect the SKA to yield new discoveries over much of the phase space depicted in Figure 2.

2.4 How Bright Can Fast Transients Be?

Some of the material here can be found in SKA Memo 97 [10].

Giant and Hyper-giant Pulses: We already know that giant pulses from certain pulsars, like the Crab, are emitted frequently enough to be detectable at plausible rates out to 1.5 Mpc with Arecibo. This number results from scaling 0.43 GHz pulses of amplitude $S_{\rm pk} \sim 150$ kJy that are pulse-broadened to $\sim 100\ \mu$s duration. Such pulses occur from the Crab at a rate $\sim 1\ {\rm hr}^{-1}$. They correspond to a pseudo-luminosity $S_{\rm pk}D^2 \sim 10^{5.8}$ Jy kpc^2. Surely there are more luminous, giant-pulse-emitting pulsars that are detectable even further.

The case can be made that there are other burst sources that can tap larger sources of free energy than are available in pulsars like the Crab. These alternatives may include:

- Pulsars born near the break-up limit (~ 1 ms) with canonical or magnetar-like magnetic fields (10^{12} to 10^{15} Gauss) can rapidly dump their rotational energy (using a moment of inertia of 10^{45} gm cm^2),

$$\frac{1}{2}I\Omega^2 = 2\pi^2 I P^{-2} \sim 10^{51.3}\,{\rm erg}\, I_{45} P_{\rm ms}^{-2}, \tag{2.8}$$

  which is comparable to the non-neutrino energy released in a supernova. This energy will be released in a short amount of time as the pulsar rapidly spins down but along the way can drive giant-pulse emission much larger than seen from the Crab, e.g. by a factor of one million, e.g $S_{\rm pk}D^2 \sim 10^{12}$ Jy kpc^2.

- Neutron stars may reactivate their magnetospheres when they merge, with orbital motion substituting for spin in the generation of voltage drops that accelerate particles and create electron-positron pairs. This kind of system is a strong candidate for "short" gamma-ray bursts. The energy involved is similar to or exceeds that for extreme giant pulse-emitting objects. The GRB peak luminosity is fiducially $L_\gamma = 10^{51} L_{\gamma,51}$ erg s^{-1}. We assume that the true radio luminosity is some multiple ε_r of this: $L_r = \varepsilon_r L_\gamma$. Remarkably, over many kinds of astrophysical objects (stars, pulsars, AGNs), we find ε_r ranging from about 10^{-8} (Crab pulsar) to 10^{-3} (blazars). Here we use a fiducial value $\varepsilon_r = 10^{-5}\varepsilon_{r,-5}$ and a radio emission bandwidth $\Delta\nu_r = 1$ GHz$\Delta\nu_{r,\rm GHz}$. We then calculate the pseudo-luminosity L_p in units of Jy kpc^2 by calculating the peak radio flux from the GRB assuming (only fiducially) isotropic emission. This gives a stupendously large pseudo-luminosity,

$$L_p = 10^{15.9}\,\mathrm{Jy\,kpc^2}\left(\frac{\varepsilon_{r,-5}L_{\gamma,51}}{\Delta\nu_{r,\rm GHz}}\right) \tag{2.9}$$

  corresponding to a peak flux density

$$S_{\rm pk} = 10^{2.9}\,\mathrm{Jy}\left(\frac{\varepsilon_{r,-5}L_{\gamma,51}}{\Delta\nu_{r,\rm GHz}}\right)\left(\frac{3\,\mathrm{Gpc}}{d_L}\right)^2. \tag{2.10}$$

  Beaming may influence the radio luminosity estimate as it does the γ-ray luminosity.

A 30 Jy pulse at 1.4 GHz has been detected that has DM$\sim$ 375 pc cm^{-3} from a direction toward which the general interstellar media in the Galaxy and the Small Magellanic Cloud cannot account for the electrons [18]. The authors argue for a 500 Mpc distance based on a 4% baryonic, ionized intergalactic medium. This corresponds to $S_{\rm pk}D^2 \sim 10^{13}$ Jy kpc^2, much larger than any known Galactic source but comparable to the maximal giant-pulse emission discussed above while being somewhat less than our estimate for prompt GRB emission (with admittedly much latitude on scaling parameters).

Scaling from the observed properties, the maximum detectable distance for the event is

$$D_{\rm max} = D\left(S_{\rm pk}/S_{\rm min}\right)^{1/2}, \tag{2.11}$$

where

$$S_{\rm min} = \frac{mS_{\rm sys}}{\left(N_{\rm pol}BW\right)^{1/2}}, \tag{2.12}$$

and $m =$ minimum S/N needed for detection, $S_{\rm sys} = \mathrm{T_{sys}/G}$ is the SEFD, $N_{\rm pol}$ is the number of polarization channels used (1 or 2), B is the bandwidth, and W is the event duration and thus the integration time (for optimal detection). For steady sources, W would be replaced with the dwell time τ used for a given pointing. In the Parkes survey that found the event $S_{\rm min} \sim 0.3$ Jy, while for Arecibo it is about 0.03 Jy, in both cases using $\tau = 5$ ms and a detection threshold $m = 10$. This means that $D_{\rm max}/D \sim 10$ for Parkes and ~ 32 for Arecibo.

A perplexing aspect of the Lorimer et al. pulse is that it is a lone event, in two senses. No other pulse was seen from the same pointing direction in many follow-up observations. Nor were weaker

— and presumably much more frequent — pulses seen from any sky position, which are expected if the pulse arose from one member of a homogeneously distributed population. The event is strong enough so that a large number of weaker events from more distant sources should have been seen. That none were (pending further reanalysis of Parkes data, PALFA data, etc.) suggests that D may be much smaller than 500 Mpc. If, for example, the source is Galactic, then $D \lesssim 10$ kpc and $D_{\rm max}$ may then be small enough that we should not expect homogeneity to hold. In this case, the absence of weaker events is not surprising.

3. Analyzing the Frequency-time Plane

All observations, whether of steady sources or the fastest transients, require processing of signals in both time and frequency. The common thread across all source types includes calibration and RFI excision. RFI, in particular, must be sampled with high resolution in the $\nu - t$ plane in order to identify its various types (narrow/broad band, impulsive, swept-frequency, etc.) and excise it.

Signal detection invariably makes use of *matched filtering* or some approximation to it. A matched filter (MF) by definition maximizes the signal-to-noise ratio of the test statistic used to define detection. MFs are used for identifying sources in images, spectral lines in spectra, pulses in time series, and more complex events in spaces of higher dimensionality. Familiar examples include identification of dispersed pulses in the $\nu - t$ plane and spectral lines with variable Doppler shifts from acceleration of the source or the observer. The MF is usually parametric; when values of parameters are not known, the MF becomes a family of filters whose performance is optimized over a grid of values.

Figure 3 shows examples of signal types in the frequency-time plane. One basic point is that, phenomenologically and topologically, a dispersed or otherwise frequency-swept signal can appear as a drifting spectral line and vice versa. An important difference of course is that the drift rates of frequency-swept pulses are typically much larger than the variable Doppler drift rates of spectral lines.

Pulse and Spectral Line Detection: For pulse detection in a time series, W_p is the characteristic width of the pulse and W_n is the characteristic time scale of the noise, comparable to the sample interval in digitized data that is Nyquist sampled. By inspection, the S/N in the time series, $S_{\rm pk}/\sigma_n$, increases by a factor $(W_p/W_n)^{1/2}$ in the MF test statistic, in accord with the expected $\sqrt{N}$ law. For a spectral line, W_p and W_n are characteristic frequency scales.

Dispersed Pulses: In the frequency-time plane, the signal shape $I(t,\nu)$ has a template that depends on the dispersion measure, DM, and on the temporal pulse width. "Post-detection" dedispersion sums over ν taking into account dispersive delays. The remaining step of matched filtering involves smoothing of the resulting time series with a filter that matches the pulse shape, $p(t)$.

A more exact method is "coherent" dedispersion [13] where the electric field is processed rather than intensity and thus involves phase as well as amplitude. Coherent dedispersion corrects the phase wrap of the signal that corresponds to the frequency-dependent time delays imposed by

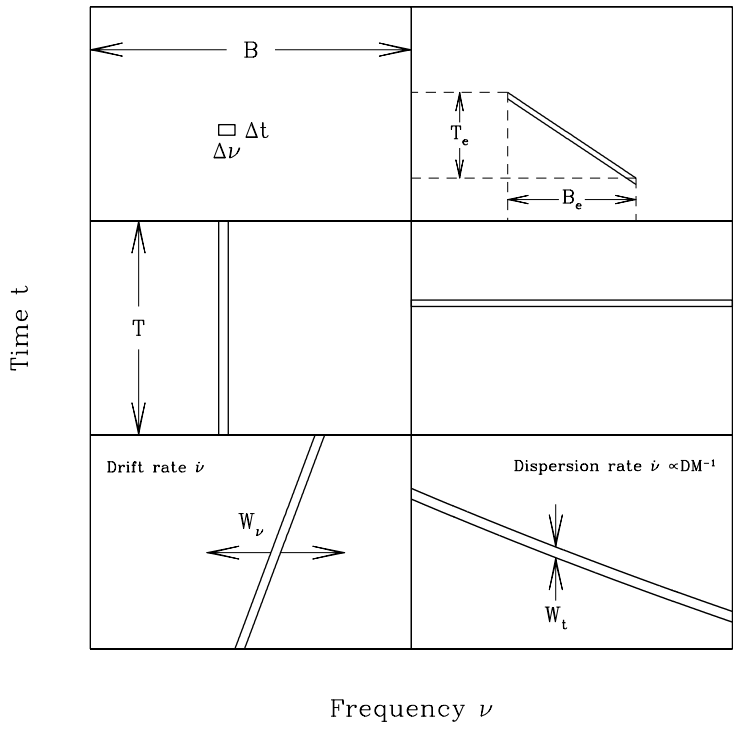

Figure 3: Schematic views of six types of signals as seen in the $\nu - t$ plane. From left to right, top to bottom we have: (a) a single cell with resolutions $\Delta\nu$ and Δt in an observational unit that spans total bandwidth B and total time T; (b) a drifting event with instantaneous widths W_ν and W_t and total spans B_e and T_e; for a uniform drift rate $\dot{\nu}$ we have $W_\nu/W_t = B_e/T_e = \dot{\nu}$; events of course may have curved trajectories in the $\nu - t$ plane; (c) a time-steady spectral line; (d) a broadband pulse; (e) a drifting spectral line with steady amplitude; (f) a dispersed pulse, including curvature of the path according to the cold-plasma dispersion law. Drifting structures as in (b), (e) and (f) may occur from processes other than those mentioned (variable Doppler shift, dispersive propagation), including refraction effects, stellar and Jovian bursts, and gravitational shifts.

dispersion. As with the post-detection method, the coherent dedispersion MF is a one-parameter filter (DM); signal detection then involves smoothing with $p(t)$, as before.

In survey applications, DM is not known *a priori*, so it becomes a parameter in a family of MFs. In applications on objects with DM known to arbitrary precision, coherent dedispersion may be viewed as exact while post-detection dedispersion is only an approximation of varying convergence to the exact case.

Pulse broadening: Multipath propagation from scattering and refraction in the ISM causes intrinsic pulse shapes $p_i(t)$ to be convolved with an asymmetric function $p_{\rm MP}(t)$ to produce $p(t) = p_i(t) * p_{\rm MP}(t)$. As above, the matched filter for detection is the measured shape $p(t)$.

Periodic Dispersed Pulses: Periodicity introduces the period P into the overall MF. For a train of pulses with fixed P and equal amplitudes, the MF is $\sum_j p(t - jP)$ e.g. [4]. The filter output over one cycle corresponds to the "folded" pulse shape often computed in pulsar applications after

smoothing by $p(t)$ to obtain maximal S/N. Search applications require a family of such rail filters with parameter P. An approximate method — widely used — consists of Fourier transformation of the time series followed by summing of harmonics for trial periods P and trial numbers of harmonics. The resulting S/N is sub-optimal because harmonic summing typically does not include phase information but can approach the MF result to within a factor $2^{-1/4}$.

Orbiting pulsars: Orbital motion causes received pulses to be unequally spaced. For orbital periods much longer than the data span of interest, a single parameter is needed — the acceleration — in the MF, which is essentially a rail filter with unequally spaced pulses. To search for objects with short orbital periods, five Keplerian parameters need to be included in the MF. Approximate methods include standard Fourier analysis on short data sets and summing of resultant spectra or analyzing orbital sidebands in the Fourier transform of the entire time series [21].

Precessing pulsars: Slowly precessing pulsars will mimic orbiting pulsars, to some extent. Objects that have complex, triaxial precession, may tumble and will defy a MF approach to an entire time series. Detection may need to rely on single-pulse detection.

ETI carrier signals: One type of proposed ETI signal is a simple carrier that drifts in frequency from accelerated motion by a drift rate $\dot{\nu}$. The MF takes into account the line width and drift rate. If the signal is transient with duration T_e, that too must be included in the MF.

Faraday rotation: Rotation of the plane of polarization by an angle $\chi \propto \nu^{-2}$RM, where RM is the rotation measure. Detection of the linearly polarized flux density is accomplished by derotating the quantity $L = Q + iU$ in the complex plane by a phase $\phi = 2\chi$ with RM an unknown parameter.

4. Radio Synoptic Surveys

Surveys of time-variable sources need to take into account event rates and durations as well as sensitivity requirements. Transients cover a very wide dynamic range in time scale. Slow transients may be sampled by raster scanning, covering a total solid angle Ω_s in a time T_s and then repeating the scan. The dwell time per sky position is $\tau = (\Omega_i/\Omega_s)T_s$, where Ω_i is the instantaneous FoV. Figure 4 shows a schematic view. Slow transients are also those for which pulse broadening from plasma dispersion and multipath propagation are unimportant. Fast transients are those that cannot be well sampled through raster-scan imaging surveys, unless they are very frequent and there is tolerance for a low survey completeness. Transients shorter than about one day qualify as fast if an all-sky survey is contemplated. Rare, fast transients are better sampled through *staring* observations of large solid angles.[3]

[3]In terms of number of detected events, it is equivalent to cover a large solid angle through raster scanning and small duty cycle per sky position, or to cover a smaller solid angle with continuous time coverage. If the goal is to characterize the angular distribution of the transient population, then raster scanning is appropriate. However, if the event rate of particular sources is desired or if the source population is restricted to a small solid angle (e.g. the Galactic center region), then staring observations are needed.

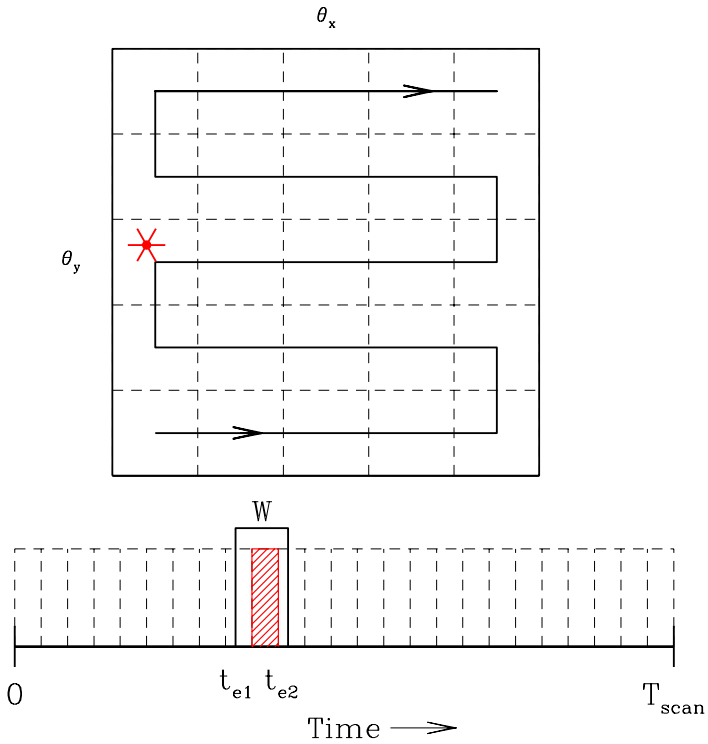

Figure 4: (Top:) Schematic view of a raster scan where each small square indicates the instantaneously sampled solid angle. The star symbol indicates the occurrence of a transient of duration W at the indicated sky position. (Bottom:) Timeline for the sampling of the event that begins at time t_{e1} during a part of the raster scan when the sky position of the transient is not in the instantaneous solid angle being sampled; the next sky position, that of the transient source, is sampled while the transient is still occuring (shaded rectangle); the transient persists while the scan samples the next sky position.

4.1 Figure of Merit for Raster-scan Surveys of Steady Sources

For blind searching, the rate of sky coverage $\dot{\Omega}$ (deg^2 s^{-1}) needs to be maximized while also achieving some desired search depth, which we characterize as the maximum detection distance, $D_{\rm max}$. Survey yield is an obvious metric and it involves the product of source number density n_s with search volume $V_s = \frac{1}{3}\Omega_{\rm s} D_{\rm max}^3$. If the survey covers total solid angle $\Omega_{\rm s}$ in a time $T_{\rm s}$, the resulting search volume yields a combination of parameters that is the same as obtained by calculating *survey speed*, $SS = \Omega_i/\tau$, but taken to a different power. The resulting figure of merit "FoMSS" (which can be read as a FoM for either steady sources or for survey speed) is

$$\mathrm{FoMSS} = B\left(\frac{N_{\rm FoV}\Omega_{\rm FoV}}{N_{\rm sa}}\right)\left(\frac{f_c A_{\rm e}}{m\mathrm{T}_{\rm sys}}\right)^2, \tag{4.1}$$

where $N_{\rm FoV}$ is the number of fields of view (or pixels) for each antenna, $\Omega_{\rm FoV}$ is the solid angle for each FoV, $N_{\rm sa}$ is the number of subarrays into which the array is divided (assumed equal in size and pointed in non-overlapping directions), f_c is the fraction of the total effective area $A_{\rm e}$ usable in the

survey, m is the threshold S/N in the survey, and $\mathrm{T_{sys}}$ is the system temperature. This expression is consistent with the simple form often used for survey speed, $B\Omega_{\mathrm{FoV}}(A_{\mathrm{e}}/\mathrm{T_{sys}})^2$, but makes manifest other variables relevant to surveys.

4.2 Figure of Merit for Pulsars ("Steady Transients")

Many pulsars, though obviously time dependent, have relatively steady pulse amplitudes. A survey metric for pulsars therefore bears some resemblance to that for steady sources, but the detectability is a function of period P and dispersion measure DM because the processing seeks harmonics of the fundamental period in a Fourier analysis of long time series.

The survey volume is $V_s = \frac{1}{3}\Omega_s D_{\mathrm{max}}^3$ with $D_{\mathrm{max}} = (L_p/S_{\mathrm{min}})^{1/2}$ as before, but now the minimum detectable flux density is written as

$$S_{\mathrm{min}}(P,\mathrm{DM}) = \frac{S_{\mathrm{min_1}}}{h_\Sigma(P,DM)}, \tag{4.2}$$

$$S_{\mathrm{min_1}} = \frac{2mk\mathrm{T_{sys}}\mathrm{N_{sa}}}{A_e\sqrt{2B\tau}}, \tag{4.3}$$

where the subscript "1" on $S_{\mathrm{min_1}}$ denotes the threshold for a single harmonic. The harmonic sum h_Σ is given by

$$h_\Sigma(P,\mathrm{DM}) = \mathrm{N_h}^{-1/2}\sum_{\mathrm{j=1}}^{\mathrm{N_h}} \left|\tilde{\mathrm{f}}_{\mathrm{j}}\right|, \tag{4.4}$$

where f_j is the Fourier amplitude (normalized to the zero frequency [$n = 0$] value so that $|f_j| \le 1$) for a time series dedispersed using dispersion measure DM; the harmonic number j corresponds to a harmonic frequency j/P of the period P; and N_h is the number of harmonics that maximizes the sum; h_Σ is equal to unity if the signal is an undistorted sinusoid but can be much larger than unity when the sum is optimized for $N_h \gg 1$. For a gaussian-shaped pulse, this number is $N_h \approx P/2W$ for a period P and pulse width (FWHM) W. If the pulse is heavily broadened by instrumental effects, scattering or orbital motion, $h_\Sigma \ll 1$ and the survey becomes insensitive.

Using these definitions, the figure of merit for a pulsar survey is

$$\mathrm{FoMPSR} = \mathrm{FoMSS} \times h_\Sigma^2(P,DM) = B\left(\frac{N_{\mathrm{FoV}}\Omega_{\mathrm{FoV}}}{N_{\mathrm{sa}}}\right)\left(\frac{f_c A_e}{m\mathrm{T_{sys}}}\right)^2 h_\Sigma^2(P,DM). \tag{4.5}$$

Comments:

1. $h_\Sigma(P,\mathrm{DM})$ is dimensionless and its square is simply a multiplier of the steady-source FoM.
2. Propagation effects (dispersion and scattering) reduce h_Σ for high-DM objects because pulses are smeared out, particularly at low frequencies; $h_\Sigma(P,\mathrm{DM})$ is therefore strongly dependent on P, DM and frequency.
3. Application of Eq. 4.5 is best done by averaging over direction, e.g. Galactic coordinates ℓ, b, for a particular survey.

4. As presented, h_Σ and FoMPSR are explicit functions of P and DM. One could alternatively define the independent variables as being P and distance, D. The corresponding DM will vary greatly for different directions, in this case. In the end it probably makes little difference as to whether DM or D is used once an average over direction is done.
5. The pulsar FoM, like the other FoMs, implicitly is based on the assumption that the population of sources is homogeneously distributed. Careful application of FoMPSR must recognize the spatial distribution of pulsars in the Galaxy and that highly sensitive surveys will reach the boundaries of the population.

4.3 Figure of Merit for Raster-scan Surveys of Transient Sources

FoMSS applies to surveys of sources that are homogeneously distributed within their spatial domain, that are standard candles, and that are time steady. It is not a good metric for transient sources. A more general metric that also applies to transients (fast or slow) is

$$\text{FoMTS} \;=\; \text{FoMSS} \times K(\eta W, \tau/W) \tag{4.6}$$

$$K(a,x) \;=\; \left(1+x^2\right)^{-1/2} \left[1-e^{-a(1+x^2)^{1/2}}\right]^{4/3}, \tag{4.7}$$

where $a \equiv \eta W$ (a measure of the overlap of events in time) is the product of event rate per source η and event duration W and $x \equiv \tau/W = \Omega_i/\dot{\Omega}W$, with $\Omega_i = N_{\rm sa}N_{\rm FoV}\Omega_{\rm FoV}$. The quantity $\dot{\Omega} = \Omega_s/T_s$ is the mean rate at which solid angle is surveyed. The factors included in $K(a,x)$ account for the integration time being determined by the transient duration (W) rather than the raster-scan dwell time τ when $W \ll \tau$ and the probability that a source is pointed at when the event occurs, assuming Poisson statistics. The function $K(a,x)$ is shown in Figure 5 and is discussed further in SKA Memo 97, Appendix A. The $K(a,x)$ factor can drastically reduce the effective survey speed from what it is for steady sources.

4.4 Completeness Coefficient of a Transient Survey

Transient sources by definition are "on" and hence detectable for only a fraction of the time, which may be small. We therefore need to consider how a survey samples a population of transient sources in both the spatial and temporal domains. A completeness coefficient C_s can be defined as the ratio of number of objects that *are* detected to the number of objects that *could be* detected during the scan time $T_{\rm s}$. For a homogeneous population of sources distributed over solid angle $\Omega_{\rm pop}$ and out to a distance $D_{\rm pop}$, this takes on the form

$$C_{\rm s} = \min\left[\frac{\Omega_{\rm s}}{\Omega_{\rm pop}},1\right] \min\left[\left(\frac{D_{\rm max}}{D_{\rm pop}}\right)^3,1\right] \frac{P_t(\eta,W,\tau)}{P_t(\eta,W,T_s)}, \tag{4.8}$$

where P_t is the temporal capture factor (the probability that at least one event occurs when the telescope is pointed at a bursting source), given by (for Poisson statistics)

$$P_t(\eta,W,\tau) = 1-e^{-\eta(W^2+\tau^2)^{1/2}}. \tag{4.9}$$

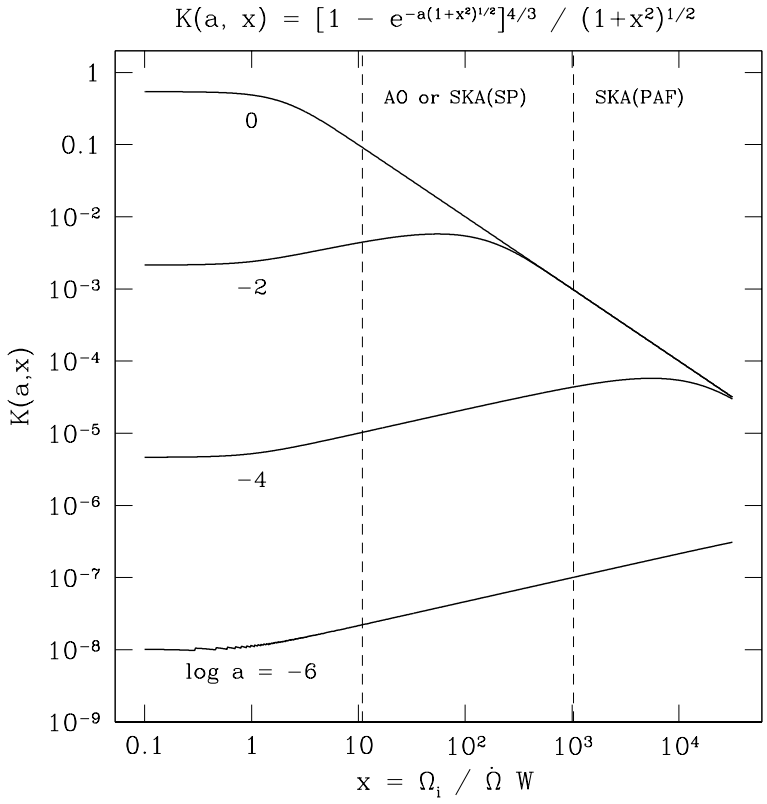

Figure 5: Plot of the temporal factor $K(a,x)$ defined in Eq. 4.7 for several values of a. The vertical lines denote values for $x = \Omega_i T_s/(\Omega_s W)$, where Ω_i is the instantaneously sampled solid angle, Ω_s is the total solid angle surveyed in time T_s, and W is the transient duration. We assume $W = 1$ s in both cases. The leftward line applies to an extragalactic survey using the 7-beam ALFA system with 3.5 arcmin beam widths at Arecibo that surveys 30% of the sky in 2000 hr. The same x is achieved for an SKA system with single-pixel feeds having 1 deg beams that survey 80% of the sky in 5 days. The line labelled "SKA(PAF)" is for the same SKA survey but using a phased-array feed with 100 beams.

There are three regimes for C_s that depend on the event rate η and on whether the events are fast or slow: $\eta W \ll \eta\tau \ll 1$, $\eta\tau \ll \eta W \ll 1$ and $\eta(W^2+\tau^2)^{1/2} \ll 1$. If there are very bright, but rare, prompt radio bursts associated with GRBs, we expect $P_t \approx \eta\tau$, and $D_{\rm max}$ to equal the population distance, in which case $C_s \approx 10^{-4}$ for an array of 10m antennas outfitted with single-pixel feeds. To detect such bursts at a reasonable rate requires a much larger field of view.

4.5 Trading Field of View and Sensitivity

The sensitivity and FoV requirements for transients can be discussed in terms of the event rate for particular classes of sources. Figure 6 shows minimum detectable flux density plotted against instantaneous solid angle. For single-reflector, single-pixel telescopes, we have a simple relationship,

$$S_{\nu,\rm min} = \frac{mS_{\rm sys}}{\sqrt{2BT}} = \frac{8k{\rm T}_{\rm sys}}{\eta_A\pi\sqrt{2BT}}\left(\frac{m\Omega_{i,1}}{\lambda^2}\right), \qquad (4.10)$$

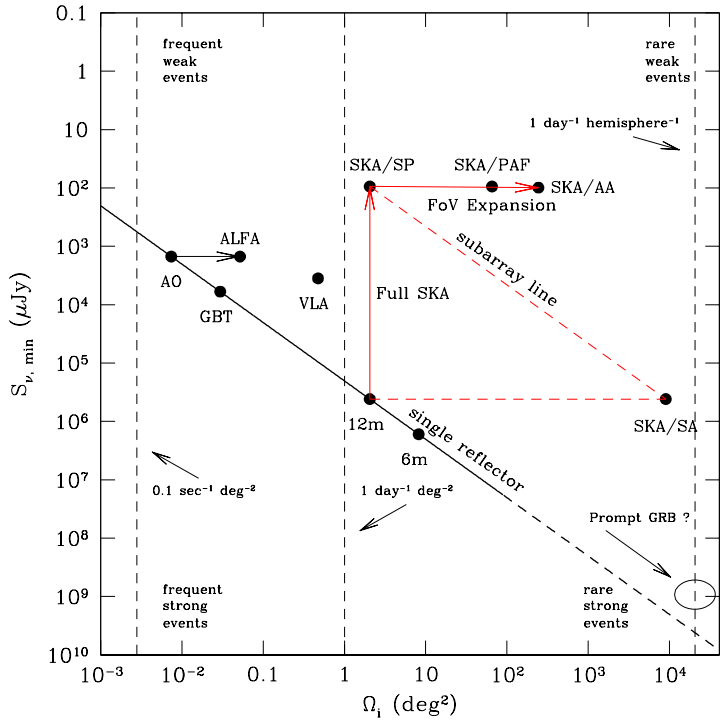

Figure 6: Plot of minimum detectable flux density ($S_{\nu,\mathrm{min}}$) vs. instantaneous solid angle Ω_i. The solid diagonal line refers to single-reflector telescopes with single pixel feeds and all having — for simplicity in presentation — the same center frequency (1 GHz), operating bandwidth (0.3 GHz), system temperature (25 K) aperture efficiency (60%), and integration time (1 s). The dashed extension of the single reflector line denotes reflector diameters $< 6\lambda$. The "Full SKA" line indicates the sensitivity for 4400 12-m antennas. "FoV expansion" implies an increase in solid-angle coverage through use of dishes + phased-array feeds (PAFs) or through an aperture array (AA). The subarray line indicates the tradeoff between sensitivity and instantaneous FoV for single-pixel systems. Vertical dashed lines indicate the solid angle needed to detect events at the indicated rates assuming a one day total exposure time. The ellipse in the bottom-right corner indicates the fiducial amplitude of hypothetical prompt radio GRB emission. The location of the GRB ellipse implies that dipole antennas may yield sufficient solid angle coverage but will be too insensitive to detect prompt GRB emission for nominal values of the burst parameters.

where the unity subscript implies a single aperture and we have assumed that $\Omega_{i,1} = (\lambda/D)^2$ (i.e. unity coefficient). The factor m, as before, is the threshold in units of the rms noise level for a bandwidth B and integration time T; the latter may or may not equal the dwell time on a given source position. The solid line in Figure 6 shows this relationship. For arrays with N_A antennas each having a multi-pixel receiver with N_{FoV} pixels, we have

$$\Omega_i = N_{\mathrm{FoV}} N_{\mathrm{sa}} \Omega_{i,1} \tag{4.11}$$

$$S_{\nu,\mathrm{min}} = \frac{1}{N_{\mathrm{a}} N_{\mathrm{FoV}}} \frac{8k\mathrm{T}_{\mathrm{sys}}}{\eta_A \pi \sqrt{2BT}} \left(\frac{m\Omega_i}{\lambda^2} \right). \tag{4.12}$$

If N_{sa} subarrays are used, the FoV increases at the expense of higher threshold. We show points in

the figure for the full SKA outfitted with a single-pixel system (SKA/SP) and with a 32-pixel system (SKA/PAF). We also show a point for an SKA built around an aperture array, which provides ~ 1 sr FoV. The slanted dashed line shows the relationship for subarrays, the ultimate configuration comprising N_A subarrays of one antenna each. The figure delineates the various permutations of strong/weak and rare/common transients. Vertical dashed lines indicate the solid angle required to capture sources of indicated event rates in a reasonable dwell time (see caption). In the figure we keep the integration time, T, fixed, as appropriate for short-duration transients with $W \ll \tau$, i.e. W shorter than the dwell time per position, in which case $T = W$. To have the temporal capture probability $P_t \sim 1$ we require, for low-rate, short-duration transients ($W \ll \tau$),

$$\Omega_i \gtrsim \frac{1}{(\eta/\Omega_s)T_s}. \tag{4.13}$$

In the figure we have considered event rates η/Ω_s of 0.1 s^{-1} deg^{-2} with a one-hour scan time and 1 day^{-1} deg^{-2} and 1 day^{-1} hemisphere^{-1} with scan times of one day for the three vertical, dashed lines from left to right. The rightmost line, for example, is relevant to the case of prompt radio pulses from GRBs, should they exist.

From the figure we can make a number of conclusions. First, if there are hyper-strong events (such as coherent radio pulses from GRBs), a wide FoV system is necessary for a reasonable detection rate, but modest collecting area may suffice for detection. However, rare weak events require high sensitivity as well as wide FoV. Field of view expansion of single reflectors allows probing of the upper right-hand corner as does an aperture array. But it is also true that wide FoV may be achieved at moderate sensitivity through the use of subarrays. Since the low-event-rate radio sky is largely unexplored, we should entertain the possibility of using the subarray approach as well as develop FoV expansion approaches.

4.6 AS vs. SA: Aperture Synthesis vs. Subarrays

It is generally more productive to use an array in aperture synthesis (AS) mode than in extreme subarray (SA) mode. Consider the case where a total time T is used to observe a region of size Ω_s. In AS mode, we fast-sample and mosaic a region of size $\Omega_s = N_p\Omega_1$ with integration time $\tau = T/N_p$ per pointing. Alternatively in an extreme subarray ("fly's eye") mode with one antenna per subarray, we would stare continuously at the same region of the sky for the same total time. Therefore the number of pointings N_p for AS equals the number of antennas, N_A. The number of events detected for transients that are fast in both AS and SA mode ($W \ll T/N_p \ll T$) is

$$\frac{N_e^{(SA)}}{N_e^{(AS)}} = N_A^{-3/2} \tag{4.14}$$

while for the case where the events are fast for SA mode ($W \ll T$) but slow for AS mode ($W > T/N_p$) we have

$$\frac{N_e^{(SA)}}{N_e^{(AS)}} = N_A^{-3/2}\left(\frac{W}{\tau}\right)^{3/4}. \tag{4.15}$$

5. The Synoptic Cycle: An Example of Multiple Commensal Surveys

Though processing requirements are challenging, there is no fundamental reason why commensal observations in a synoptic survey mode with the SKA (and precursor instruments) cannot provide a massive survey of HI in galaxies, large numbers of Faraday rotation measures, a full-Galactic census of pulsars, and unprecedented characterization of the transient radio sky that, together, are the basis for profound progress in fundamental physics, cosmology, astrophysics and astrobiology as well as providing discoveries of entirely new sources and phenomena.

The observing cycle for a given survey consists of a raster scan of a region of sky Ω_s in a time T_s, yielding a dwell time per sky position $\tau = T_s\Omega_i/\Omega_s$. In practice this rate may be achieved by continuous scanning or by dwelling on each of a predefined grid of positions. This cycle can be repeated many times, allowing detection of a growing number of transient sources, both periodic ones like pulsars and magnetars, and one-shot objects like GRBs. At the same time, signal-to-noise ratio is built up for steady sources, such as HI in galaxies, continuum sources for AGN surveys and Faraday rotation measurements. Because multiple surveys are potentially doable, and each is demanding on total telescope time, all effort should be made to do the surveys simultaneously (commensally).

To accomplish multiple surveys, a hierarchical approach to scanning rates (or cadences) is probably needed. A fast rate is appropriate for the extragalactic sky in order to sample GRB afterglows while also building S/N on HI galaxies. A slower rate is needed for the Galactic disk to provide adequate time series durations for pulsar surveys. Staring observations of the Galactic center source will allow deep pulsar and transient surveys from the star cluster. Finally, guest-investigator experimental or one-time observations need to be accomodated along with target-of-opportunity observations as they arise.

An example scenario includes both fast and slow scanning observations and staring observations. This example sums to about 10 days per cycle, which would be repeated as needed:

1. **Fast scan of the extragalactic sky:** large-scale galaxy HI survey, Faraday rotation survey, AGN survey, transients and high-latitude pulsars (millisecond pulsars and those in relativistic binaries with NS or blackhole companions):
   (a) "Full sky" survey (80% of 4π) using a 1 deg^2 FoV single pixel system
   (b) $T_s = 5$ days to cover one scan of the sky
   (c) $\tau \approx 10$ s dwell time per sky position
   (d) $S_{\rm min} \approx (g_\theta f_c)^{-1} 15$ μJy at 10σ where f_c is the fraction of a full SKA available and $g_\theta \leq 1$ is the gain relative to the on-axis gain
   (e) Field-of-view expansion through multiple feed clusters or phased-array feeds will increase the sensitivity for fixed T_s; aperture arrays would also provide an increase. A thirty-beam phased-array feed, for example, would yield 300 s dwell time
   (f) Subarrays will reduce the sensitivity but can cover more instantaneous solid angle and reduce T_s.

   (g) Commensal observations require appropriate real-time, backend processing systems that will cost a significant fraction of the overall cost of a synoptic telescope.

2. **Slower scan or staring observations on deep extragalactic fields** e.g. 1 day
3. **Slower scan for the Galactic plane:** pulsars, masers, transients, ETI sources, etc. e.g. 1 day scan of the inner Galaxy (180 deg in longitude) in a ± 1 deg swath in Galactic latitude, yielding 240 s per pointing

   (a) A *minimum contiguous dwell time* is needed for pulsar surveys that use Fast Folding Algorithms or Fourier transforms of a contiguous time series combined with harmonic summing (100 to 1000 s typical); single-pulse searches do not place strong requirements on contiguous blocks.
   (b) Pulsar timing: frequent re-observations are needed for long-term monitoring; a 10-day cadence is acceptable, so that timing measurements can be obtained as part of the survey.

4. **Staring observations:** e.g. 12 hr on the Galactic center for to detect pulsars and transients.
5. **Break out for targeted observations by individual investigators:** 10% of the time?
6. **Break out for targets of opportunity:** e.g. GRB triggers, blazar observations, etc. 5% of the time?
7. **Calibration allowance**

Additional comments on this scenario are as follows:

1. The distinction between "survey" and "follow up" observations is fuzzy. For example, timing observations of known and new pulsars can be obtained using the same survey scans that yield detections of new sources.
2. HI detection of galaxies at $z \sim 1$ requires many hours of integration time, which would build up slowly unless there is field-of-view expansion.
3. Pulsar surveys can accumulate S/N through incoherent summing of power spectra from non-contiguous data segments, with due allowance for acceleration of the source or observer. Coherent sums across multiple days are probably too demanding computationally, but with requirements that depend on the cadence.
4. Diffractive and refractive interstellar scintillations (DISS and RISS) will modulate compact sources to varying degrees and with a wide range of correlation times. To optimize detection, multiple passes on the same sky position should be uncorrelated with respect to DISS and RISS [7].

6. Processing Requirements

The processing requirements for surveys that aim to detect steady sources along with slow and fast transients, including pulsars, are severe. On a per-pixel basis, current pulsar surveys with several

hundred channels over bandwidths of 0.1 to 0.3 GHz recorded every 64 μs, the data rate is about 10 MB s^{-1}. Arrays of dish antennas with diameter D over a maximum baseline $b_{\rm max}$ require $N_{\rm pix}$ pixels to cover the solid angle encompassed by the main lobe of the primary beam pattern of each antenna, where

$$N_{\rm pix} \approx 10^{3.8} \left(\frac{b_{\rm max,km}}{D_{12}} \right)^2 \tag{6.1}$$

for a 1-km diameter array and 12-m diameter antennas. For each pixel a full pulsar/transient analysis is needed. However, the operations count is dominated by the processing needed to form data streams for each pixel prior to the post processing. These can be constructed either by calculating Fourier images from complex visibilities calculated on all baselines or by direct beam forming, with the correlation approach favored if the full field of view is to be processed.

To pursue synoptic capabilities of pathfinder arrays and the SKA, consideration must also be made of calibration requirements and RFI excision, as well as the particular algorithms needed for signal detection for the varied source classes described above. Due consideration also is needed for which part of the processing must occur in real time, in balance with long-term storage of sufficient data products to allow future data mining with new algorithms.

Acknowledgments

I thank R. Bhat, G. Bower, B. Boyle, J. Deneva, R. Ekers, D. Frail, P. Freire, B. Gaensler, T. Hankins, M. Haynes, K. Kellerman, M. Kramer, S. Kulkarni, J. Lazio, D. Lorimer, A. Lyne, J-P. Macquart, M. McLaughlin, S. Myers, R. Schilizzi, R. Shannon, I. Wasserman, D. Werthimer and P. Wilkinson for useful discussions.

References

[1] C. Akerlof et al., *Observation of Contemporaneous Optical Radiation from a Gamma-ray Burst*, *Nature*, **398**, (400) 1999

[2] G. C. Bower et al., *A Radio Transient 0.1 Parsecs from Sagittarius A*, ApJ*, **633** (218) 2005

[3] G. C. Bower et al, *Submillijansky Transients in Archival Radio Observations, ApJ*, **666** (346) 2007

[4] W. R. Burns & B. G. Clark, *Pulsar Search Techniques*, *Ast Ap*, **2** (280) 1969

[5] F. Camilo et al., *Transient Pulsed Radio Emission from a Magnetar*, 2006, *Nature*, **442** (892) 2006

[6] F. Camilo et al., *1E 1547.0-5408: A Radio-emitting Magnetar with a Rotation Period of 2 Seconds, ApJL*, **666** (93) 2007

[7] J. M. Cordes & T. J. W. Lazio, *Interstellar scattering effects on the detection of narrow-band signals, ApJ*, **376** (123) 1991

[8] J. M. Cordes & T. J. W. Lazio, *NE2001. I. A New Model for the Galactic Distribution of Free Electrons and its Fluctuations* [astro-ph/0207156]

[9] J. M. Cordes, T. J. W. Lazio & M. A. McLaughlin, *The Dynamic Radio Sky*, *New Astronomy Review*, **48** (1459) 2004

[10] J. M. Cordes, *The Square Kilometer Array as a Radio Synoptic Survey Telescope: Widefield Surveys for Transients, Pulsars and ETI*, SKA Memo 97, http://www.skatelescope.org, 2007

[11] D. A. Frail et al., *An Energetic Afterglow from a Distant Explosion*, *ApJL*, **646** (99) 2006

[12] G. Hallinan, et al., *Periodic Bursts of Coherent Radio Emission from an Ultracool Dwarf*, *ApJL*, **663** (25) 2007

[13] T. H. Hankins, *Microsecond Intensity Variations in the Radio Emissions from CP 0950*, *ApJ*, **169** (487) 1971

[14] T. H. Hankins & J. A. Eilek, *Radio Emission Signatures in the Crab Pulsar*, *ApJL*, **670** (693) 2007

[15] B. M. S. Hansen & M. Lyutikov, *Radio and X-ray Signatures of Merging Neutron Stars*, *MNRAS*, **322** (695) 2001

[16] S. D. Hyman et al., *A New Radio Detection of the Transient Bursting Source GCRT J1745-3009*, *ApJ*, **639** (348) 2006

[17] M. Kramer et al.. *A Periodically Active Pulsar Giving Insight into Magnetospheric Physics*, *Science*, **312** (549) 2006

[18] D. R. Lorimer et al., *A Bright Millisecond Radio Burst of Extragalactic Origin*, *Science*, **318** (777) 2007

[19] J.-P. Macquart, *On the Detectability of Prompt Coherent Gamma-Ray Burst Radio Emission*, *ApJL*, **658** (1) 2007

[20] M. A. McLaughlin, et al., *Transient Radio Bursts from Rotating Neutron Stars*, 2006, *Nature*, 439, 817

[21] S. M. Ransom, J. M. Cordes & S. S. Eikenberry, *A New Search Technique for Short Orbital Period Binary Pulsars*, *ApJ*, **589** (911) 2003

[22] B. J. Rickett, *Radio Propagation Through the Turbulent Interstellar Plasma*, *ARAA*, **28** (561) 1990

[23] P. Wilkinson et al., *The Exploration of the Unknown*, *New Astronomy Review*, **48** (1551) 2004